ANALYSIS OF HYSTERETIC BEHAVIOR OF TWO-DOF SOFT ROBOTIC ARM

ALEXANDER HOSOVSKY, JAN PITEL, KAMIL ZIDEK

Faculty of Manufacturing Technologies with seat in Presov
Technical University of Kosice, Presov, Slovak Republic

DOI: 10.17973/MMSJ.2016_09_201625

e-mail: alexander.hosovsky@tuke.sk

Soft robotic arm actuated with pneumatic artificial muscles (PAMs) exhibits various interesting properties (static or dynamic) in contrast to conventional robots with electric motors. In addition to nonlinear relationship between various variables, PAMs are known for the hysteresis inevitably associated with their specific construction. In order to be able to develop a model useful for designing the effective control, it is necessary to analyse the relevant features of its performance. In particular, we concentrate on analysing certain aspects of hysteretic behaviour of two-DOF planar arm which uses two pairs of PAMs so that the results can be used e.g. for compensation of hysteresis using its inverse model.

KEYWORDS

dynamic model, pneumatic artificial muscles, robotic arm, joint angle, hysteresis

1 INTRODUCTION

Pneumatic artificial muscles (PAM) experienced renewed surge of interest from the researchers in 1980s when technological advances in several fields made it possible to construct practical actuators. Since then, several various designs appeared which differ in their properties but not in their fundamental principle of operation. PAMs are pneumatic devices consisting of a rubber tube surrounded with an inextensible braided shell made of e.g. nylon or aramid fibres. When inflated, the PAMs contract axially and extend radially while simultaneously generating an unidirectional force in axial direction. Due to their specific construction they are known for their remarkable power/weight ratio, natural compliance, low overall weight and clear operation. On the other hand, they are inherently nonlinear and exhibit hysteretic behavior which are the features that make modeling and control design much more challenging. Investigation of static and dynamic properties of PAMs and the derivation of their models was the subject of research in many papers, e.g. [Doumit 2009], [Hildebrandt 2005], [Schreiber 2012], [Wickramatunge 2009], [Van Damme 2008]. An exhaustive review of state-of-the-art research on the modeling of PAMs can be found in [Tondu 2009]. In addition to works dedicated to modeling (and possibly control) of a single pneumatic artificial muscle, a lot of research has been devoted to mechanisms of various kinematic configuration actuated by PAMs, e.g. [Zhu 2008], [Ahn 2010], [Kecskemethy 2008], [Pujana-Arrese 2010]. Using any of the aforementioned approaches to PAM modeling, a suitable model for control design could be derived which was almost invariably of nonlinear type, e.g. [Hildebrandt 2005], [Lin 2015], [Schindele 2013], [Schreiber 2012], [Zhang 2008], [Zhong 2014]. With regard to attempts to design effective control for PAM-based systems, an issue of hysteresis modeling might be of great importance.

In [Vo-Minh 2009] the hysteretic behavior of PAM is investigated and found to be similar to a presliding regime in the friction of mechanical elements. In [Vo-Minh 2011] the same group of researchers also presented a model of PAM hysteresis using the Maxwell-slip model, where the hysteresis is modeled using several Maxwell-slip elements each with different stiffness and saturation force. This model was then used for hysteresis compensation using the feedforward control. A different and interesting approach was presented in [Lin 2015], where Prandtl-Ishlinskii model of hysteresis was used again for hysteresis compensation using the feedforward control. A similar approach using P-I hysteresis model (yet in the form of asymmetric shifted P-I model or ASPI) was used in [Schindele 2012], which was subsequently used for hysteresis compensation in the backstepping control. In a more generally oriented paper (from hysteresis modeling viewpoint) [Aschemann 2014], the comparison of three different hysteresis models (Bouc-Wen, Prandtl-Ishinskii and Maxwell-slip) is made. In addition to the abovementioned hysteresis models, one of the commonly used in the area of SMA or piezoelectric actuators is Preisach hysteresis model, which was also used for hysteresis modeling in [M. van Damme 2008] for a special type of pleated pneumatic muscles.

Our objective in this paper is to investigate some properties of the hysteresis of 2-DOF planar arm. In the initial phase of research, we concentrated on the examination of dynamic hysteresis of one joint, so that the results were not distorted by the dynamic joint coupling. Based on these results, appropriate inverse hysteresis model will be selected which, in turn, will be used for the calculation of proper pressure difference based on the desired joint position.

2 HYSTERESIS IN TWO-DOF SOFT ROBOTIC ARM

A system with hysteresis can be described as a system with memory, where the current output of the system depends not only on the current input but also on the history of input values up to the current time [hysteresis in magnetism]. We can see the general form of non-local hysteresis with minor loops in Fig.1. If we suppose that both input and output are zero at time $t = 0$ ($x_0 = y_0 = 0$) and input is increased to value x_1, the output follows the red curve called virgin curve. The input value x_2 corresponds to a maximum input value and if the input is reduced from this point, output starts to follow the outline of the major loop shown in green until the minimum value of input is attained. After increasing the input again to value x_3', we might start reducing the input (through value x_3) and the minor loop trajectory (shown in purple) is followed. It should be noted that the formation of minor loops is typical yet not necessary characteristic of hysteresis [Mayergoyz 2003].

With regard to the complexity of hysteretic behavior, there are two types of hysteresis: local and non-local [Riccardi 2012]. For local hysteresis, a pair of initial values $x_0, y_0 \in \Omega$ (where Ω is a hysteretic region formed by the major loop) and $x(t)$ for $t > t_0$ completely and uniquely determines the output $y(t)$. Thus, the local hysteresis can be described as

$$y(t) = \Gamma[x; x_0, y_0](t) \tag{1}$$

where $x_0 \in \Re$, $y_0 \in \Lambda(x_0)$ and $t \geq t_0$. In the equation above, Γ is hysteretic operator and Λ is output admissible set.

In case of non-local hysteresis it is not possible to determine future output based on the knowledge of $x_0, y_0 \in \Omega$ and $x(t)$ only, but also previous values of $x(t)$ for $t < t_0$ are needed.

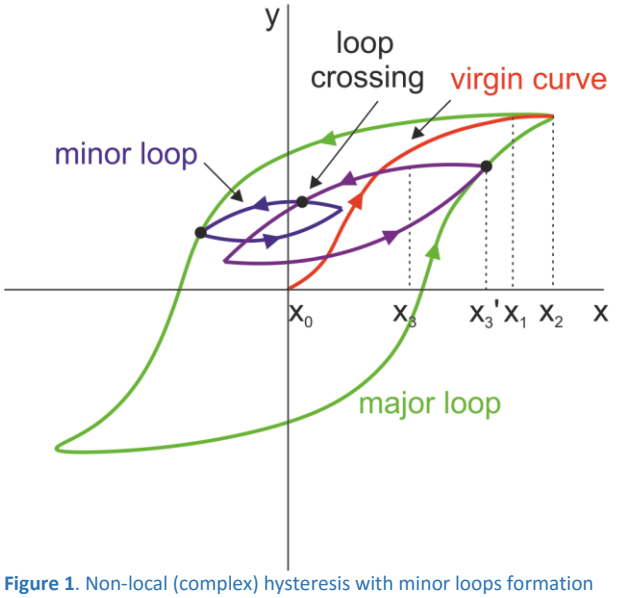

Figure 1. Non-local (complex) hysteresis with minor loops formation

This can be expressed through the state vector *z*, so

$$y(t) = \Gamma[x; z_0](t) \tag{2}$$

where $z_0 \in \Re^n$, n – state vector dimension.

The nonuniqueness of the future evolution of hysteresis output based on the initial and current values of input only can be seen in Fig.1 when the crossing of two minor loop occurs. At this point, the output will follow the curve that is determined by the previous history of input values.

The possible source of hysteresis in PAMs are given in [Vo-Minh 2011] and they include: strands friction due to their mutual contact, friction between strands and bladder, conical deformation and bladder stretching due to volume increase. In [Tondu 2009] the strand-on-strand contact is mentioned as the most probable cause of hysteresis in PAMs. On the other, it is shown in [Bergemann 2002] that the construction of Fluidic muscle prevents the contact between strands due to their separation in radial direction and therefore the remaining mentioned sources may be more probable in this case.

Since we are interested in hysteresis of θ - Δp relationship (joint angle – pressure difference), its origin can be identified with the hysteresis of force function of each of the muscles. In Fig.2 we can observe the static force characteristics of antagonistic pair of two muscles with one-muscle control. If both muscles are initially pressurized to almost maximum pressure (550 kPa), depressurizing one of them can be used for controlling the joint angle.

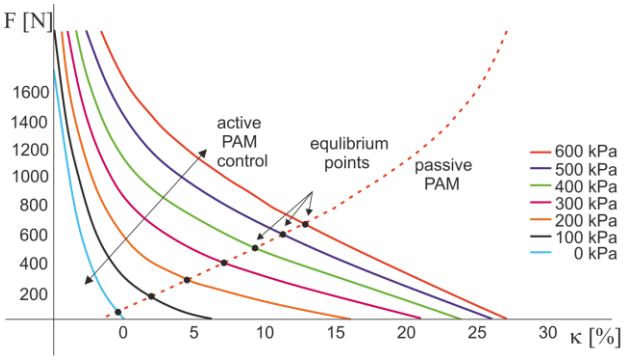

Figure 2. Static force characteristics of antagonistic pair of PAMs with one-muscle control

The force of PAM is a nonlinear function of its pressure P_m and contraction κ:

$$F_m = f(P_m, \kappa) \tag{3}$$

where muscle contraction is related to its length in the following way:

$$\kappa = \left(1 - \frac{l}{l_0}\right) = (1 - l_r) \tag{4}$$

where l_0 – initial muscle length (when unpressurized) and l_r – relative muscle length.

The static torque of a PAM pair (T_j) can be given as a difference of muscle forces multiplied by the sprocket diameter (r):

$$T_j = [F_{m1}(P_{m1}, \kappa_1) - F_{m2}(P_{m2}, \kappa_2)]r \tag{5}$$

When in equilibrium, the muscle pair has to generate sufficient torque to compensate for a gravity torque, magnitude of which depends on mechanical parameters of the robot arm and its position:

$$\begin{aligned} \Delta F_1 &= [(m_2 l_1 + m_1 c_1)\cos\theta_1 + m_2 c_2 \cos(\theta_1 + \theta_2)]k, \\ \Delta F_2 &= m_2 c_2 \cos(\theta_1 + \theta_2)k, \end{aligned} \tag{6}$$

where $k = g/r$ and g – gravity constant. As the torque of a muscle pair is proportional to the force difference ΔF and the muscle force itself depends on muscle pressure, it can be stated that the torque (and also the joint angle) is proportional to the muscle pressure difference ΔP_m:

$$T_j \propto \Delta P_m \tag{7}$$

Fluidic muscle manufacturer (FESTO) gives maximum hysteresis for muscles with diameter of 20 mm as 2.5% of nominal length. If we consider a nominal length of 250 mm (our case), this translates to a maximum hysteresis of 6.25 mm. When dealing with the worst-case scenario (and neglecting all other factors), we obtain a maximum figure of 12.5 mm of hysteresis for each of the antagonistic pairs which, when expressed as a joint angle, equals:

$$\theta = \frac{\Delta l_m}{r} = \frac{0.0125}{0.035} = 0.357 rad \tag{8}$$

This figure (approximately 20°) is quite significant compared to the maximum range of movement for both joints.

3 DESCRIPTION OF THE SYSTEM

In our experiments, we used a two-DOF robotic arm with two rotational joints. The arm itself was attached to an upper base which, in industrial implementation, would correspond to a special type of ceiling-mounted robots [Jazar 2010]. Each rotational joint was actuated with two pairs of PAMs from FESTO (MAS-20), each with a length of 250 mm and a diameter of 20 mm. The torque developed by antagonistic action of both muscles was transferred to the joint using a chain and sprocket mechanism. The joint angle was in both cases measured using Kubler 3610 optical encoders with resolution of 2500 pulses/rev. The signals from the encoders were fed to the PC using I/O card Humusoft MF624 with dedicated encoder inputs.

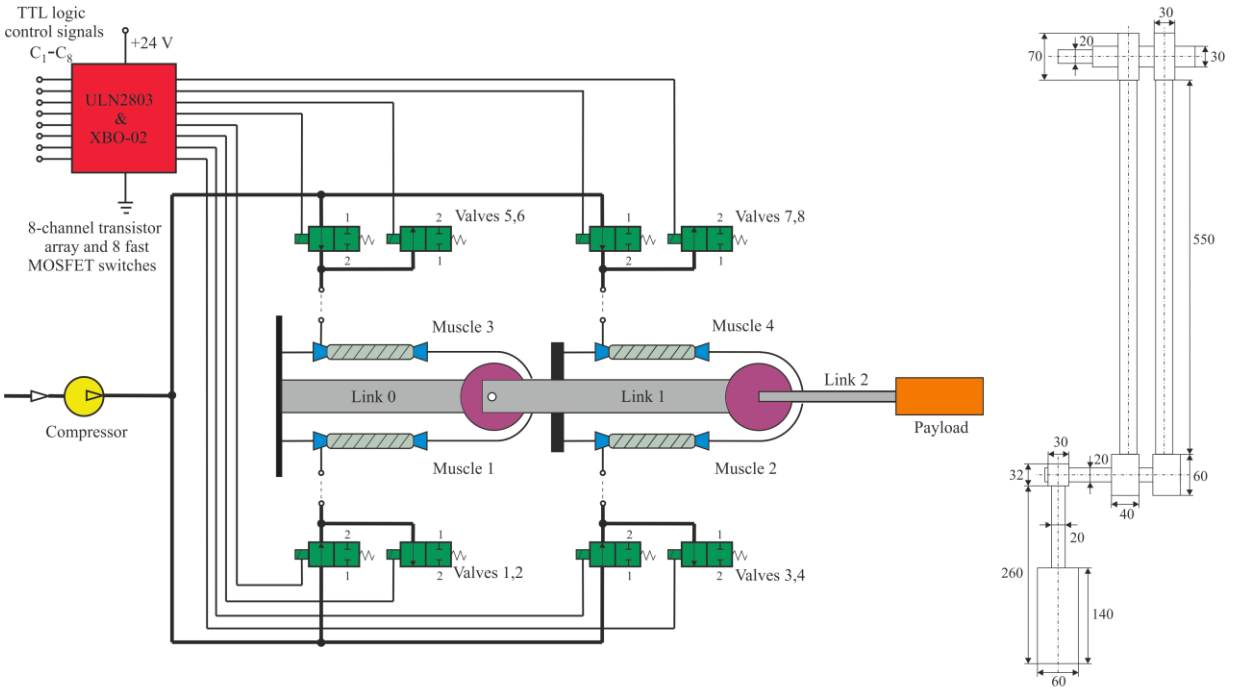

Figure 3. The basic diagram of two-DOF soft robotic arm containing the main control elements (left) and the dimensions of the robotic arm (right)

The output from the PC was in the form of digital signal used for controlling Matrix 821 on-off valves. In the power electronics part of the system, 8-channel transistor array (ULN2803) and eight fast MOSFET switches (ELSACO XBO-02) were used for powering the valves. The control of the system as well as all necessary processing of relevant data were carried out in Matlab/Simulink environment.

We can see the basic diagram of the system depicting all important system components in Fig.3. In the right part of picture, the dimensions of the manipulator are shown. The link 2 is ended with a detachable cylinder, which represents a load with certain moment of inertia. Since in this paper we are dealing with static hysteresis of the system, we do not take into account the differences in dynamics caused by the changes in moment of inertia and all the measurements were carried out with the cylinder fixed at place. The photo of actual two-DOF soft robotic arm with the main components of mechanical structure and control system is shown in Fig.4.

4 EXPERIMENTAL PART

Due to the use of on-off valves, the system is controlled using appropriate digital signal from PC equipped with data acquisition card (Humusoft MF624). The total number of valves was eight, so the 8-bit digital control signal was used with logic 0 corresponding to closed state and logic 1 to open state of a given valve. In this phase, we have investigated only the hysteresis of one joint (bottom axis) since the effect of dynamic coupling between the joints precluded undistorted measurements of the hysteresis.

The function we are interested in is the dependence of joint angle (θ) on the difference of pressure in both PAMs (Δp). This relationship can be measured by measuring the joint angle using an encoder while controlling the pressure in muscles in alternating manner. The control logic for this movement of the joint is shown in Tab.1. As we are controlling only one joint (and assuming we use one-muscle control scheme), only one logic signal would be sufficient for a given direction of the joint rotation. Actually, two logic signals are used to achieve a smooth transition through the zero-angle position (after that point a logic one for different valve is needed). Thus, for clockwise rotation we used a signal causing muscle 2 to pressurize and muscle 4 to depressurize. On the other hand, for counterclockwise direction, muscle 2 is depressurized while muscle 4 is pressurized.

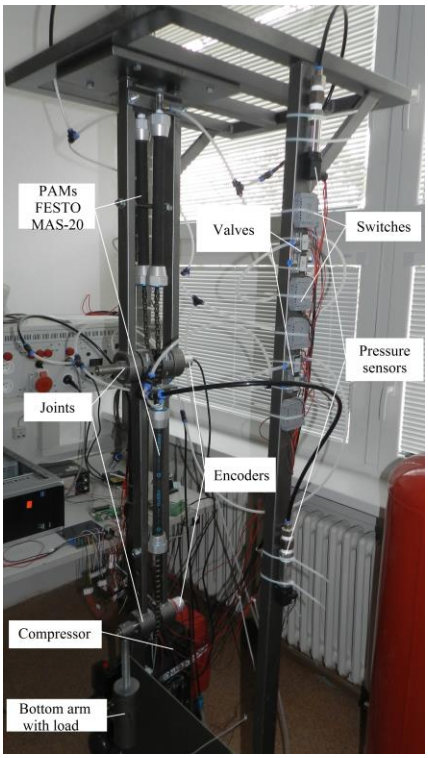

Figure 4. PAM-actuated 2-DOF soft robotic arm

If simple on-off valves are used, pressure difference as an input variable in θ - Δp relationship is not controlled directly but in response to a control signal, which opens a given valve for muscle pressurization or depressurization.

Table 1. Joint movement direction control (D – rotation direction, V1 – V8 – control signal for valve 1..8)

D	V1	V2	V3	V4	V5	V6	V7	V8
CC	0	0	1	0	0	0	0	1
CCW	0	0	0	1	0	0	1	0

To achieve the hysteresis looping, a pulse train with certain frequency was used. The correspondence between the pulse train frequency and resulting pressure difference variation is shown in Fig.5. It is obvious that there is an inverse relationship between the frequency of control signal and the amplitude of pressure difference variation. It is of note that the pressure difference waveform is not necessarily triangular in its shape, especially for larger amplitudes. This can be attributed to the physical condition of empty PAM at either end of the major loop.

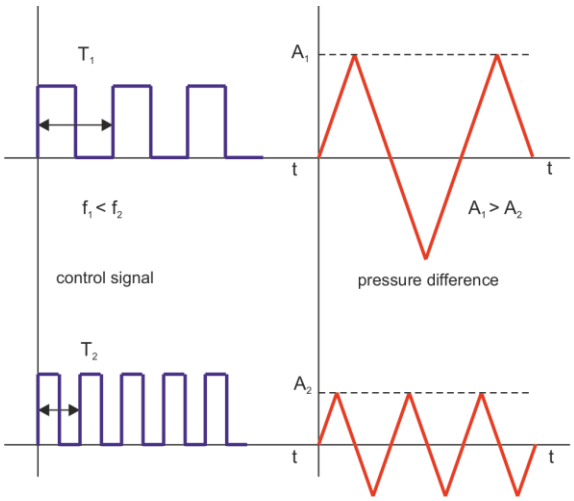

Figure 5. Relationship between control signal frequency and amplitude of pressure difference variation

Firstly, we investigate the formation of major loop in θ - Δp relationship. A signal with frequency of 0.2 Hz, which provided the excitation of robot joint through a full range of joint angle was used (Fig.6). The maximum and minimum values correspond (in absolute value) to a maximum pressure difference for given configuration, i.e. 571.88 kPa. These values also coincide with the end points of major loop in Fig.7. As can be clearly seen in this figure, the output follows the virgin curve which starts at the origin of θ - Δp coordinate system and represents the set-up position of robot joint. After reaching the end point of virgin curve (one of the PAMs is fully depressurized), the output starts to follow major hysteresis loop if it continues to be excited by signal with the same frequency. The hysteresis is widest at zero pressure difference where its width stretches from +11.5° to -11.5°. As mentioned above, the shape of pressure difference waveform is not triangular in this case due to the more gradual pressure change in muscles when the state of complete depressurization is reached.

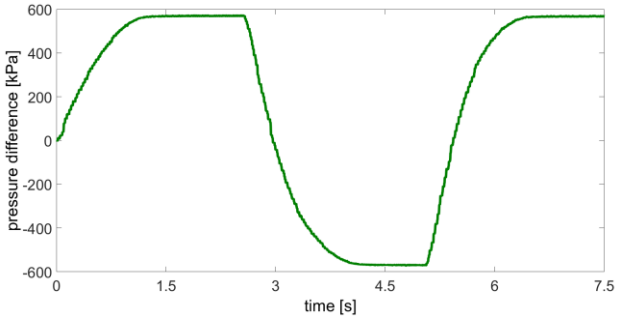

Figure 6. Time dependence of pressure difference for one major loop cycle with the input signal frequency of 0.2 Hz

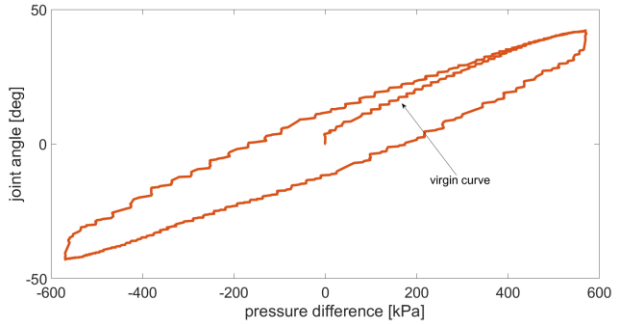

Figure 7. Major loop hysteresis with virgin curve from the set-up position

In the second experiment, we tried to combine the formation of major loop with minor loop using the switch from signal with 0.2 Hz to a signal with higher frequency (1 Hz). The result can be seen in Fig.8 and Fig.9. The first part of the pressure difference waveform is similar to Fig.6, where it was used for the formation of major loop. This waveform is interrupted in t = 8 s, where the excitation signal frequency is switched to a higher value. We can observe the formation of several minor loops in Fig.9, which are in accordance with pressure difference waveform from the point of frequency switching. The output diverges from major loop at p_D = -110.2 kPa and follows the minor loop formed by the pressure difference variation from -110.2 kPa to 309.9 kPa at first triangular peak. It is clear that constant frequency of the pulse excitation signal is not necessarily translated into a pressure difference waveform with constant amplitude. This can be possibly explained through the robot arm dynamics (reaction torques) affecting the pressures in PAMs. As soon as the pressure difference waveform is stable in its amplitude (third and fourth peak in Fig.8), the output forms the same minor loops (third- and fourth-period minor loop in Fig.9).

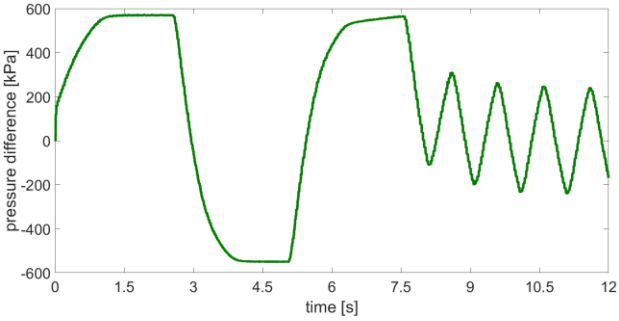

Figure 8. Time dependence of pressure difference for switching from major loop to minor loop cycling with the input signal frequency 1 Hz

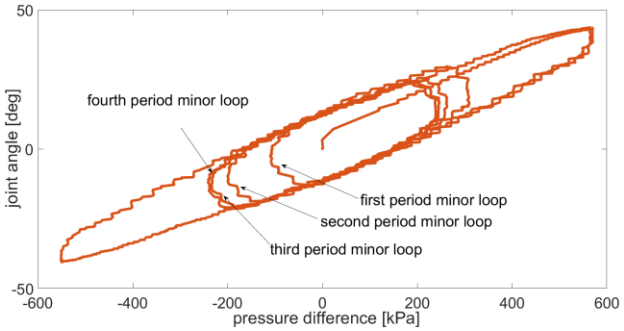

Figure 9. Stabilization of minor loop formation using the pressure difference input with constant amplitude

In the third experiment we tested the combination of major loop formation and two minor loops generated by the pulse trains with different frequencies. The pressure difference waveform for this test is shown in Fig.10. The waveform starts with the pressure difference corresponding to a signal with frequency of 0.2 Hz. In t = 13 s, the frequency of the pulse train is changed to 1 Hz and in t = 26 s to 2 Hz. It is readily observable that due to the aforementioned reasons, it was not possible to achieve the constant amplitude of pressure difference waveform. Moreover, the switch point at which the frequency of pulse train was changed could significantly disturb the uniformity of the waveform (second switch point at 26 s). The result of this is the formation of multiple minor loops only slightly shifted in the direction of x-axis (Fig.11). Ideally, the pulse signals with constant frequency would result in the formation of exactly one minor loop.

For the waveform shown in Fig.10, the average value (N = 10) of peak-to-peak pressure difference for the excitation signal with frequency of 1 Hz (from t = 13 s to t = 26 s) was 545.48 kPa with standard deviation of 5.08 kPa. In case of f = 2 Hz (N = 14), the average value was 254.8 kPa with standard deviation of 8.56 kPa. Further experiments also confirmed the fact that the uniformity of pressure difference waveform amplitude is more severely compromised for higher frequencies of excitation signal.

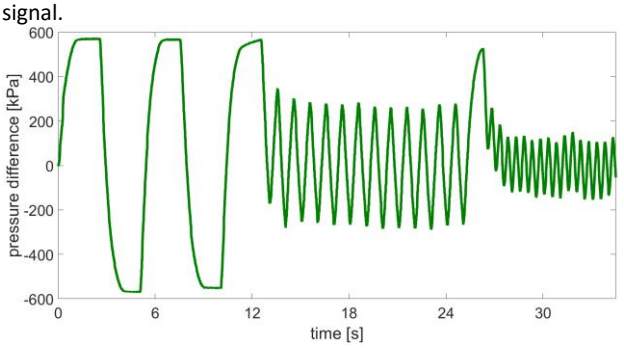

Figure 10. Time dependence of pressure difference for switching from a major loop to 2 minor loops cycling with the input signal frequency of 1 Hz and 2 Hz

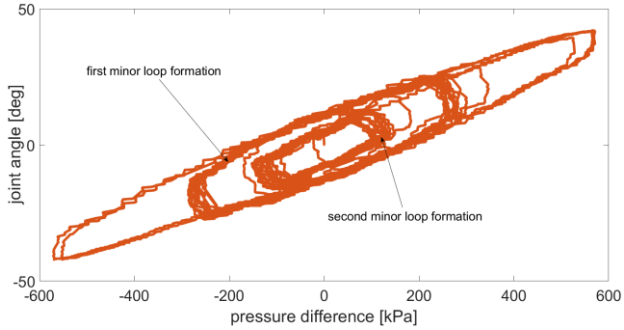

Figure 11. Formation of two minor multiloops using the pressure difference input with two different amplitudes

To test the formation of hysteresis output for arbitrary excitation signal, we selected a signal with random variation of pulse durations as well as their position in time. This signal was used in the time range of 30 seconds and its form is shown in Fig.12. A blue color was used for signals fed to valves 3 and 8 (pressurization valve for the second muscle and depressurization valve for the fourth muscle respectively) and red color for signals fed to valves 4 and 7 (depressurization valve for the second muscle and pressurization valve for the fourth muscle respectively). As mentioned previously, the control signal shown in the figure is fed simultaneously to given valve combinations in order to achieve smooth transition through the zero position.

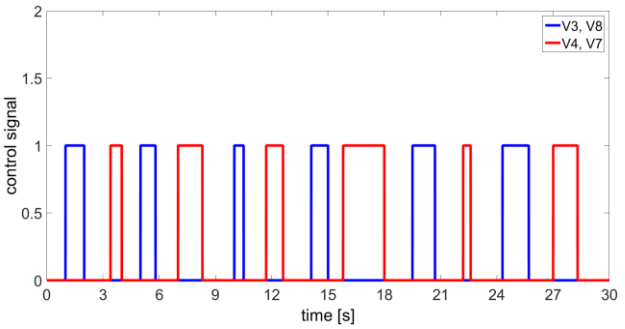

Figure 12. Excitation signal in the form of pulses with randomly chosen duration and position in time

The pressure difference waveform for the signal shown in Fig.12 is depicted in Fig.13. The system started again from the set-up position with the pressure difference of 0 kPa. In this experiment the formation of major as well as several minor loops can be observed (Fig.14). In addition to that, the presence of minor loops crossing is now easily discernible. This attests to the fact that the hysteresis of θ - Δp relationship in 2-DOF PAM-based robotic arm has non-local character and the future value of its output from a given point depends not only on the starting point and the current but also on the history of input values.

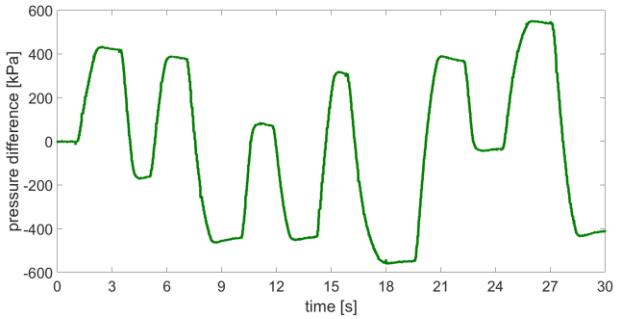

Figure 13. Pressure difference waveform for the excitation with random pulses

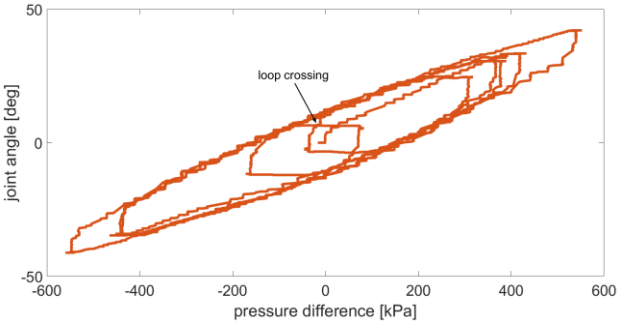

Figure 14. Non-local hysteresis in θ - Δp relationship obtained using the random pulse excitation

From quantitative viewpoint, the results obtained from the experiments are more or less in accordance with the expectations based on the data from manufacturer (maximum width of the hysteresis for joint angle was 23° compared to expected 20° – Eq.8). Of the note is also the shape of minor loops for lower frequencies, which basically resemble the major loop albeit with smaller range in the x-axis direction. This points to the fact that the width of hysteresis was roughly comparable. On the other hand, for a higher frequency (2 Hz – Fig.11) we can observe decrease in the ranges for both axes directions. This can be possibly attributed to the specific properties of hysteresis of force function of PAMs themselves.

5 CONCLUSION

In the paper we have analyzed certain properties of the hysteretic behavior of θ - Δp relationship in 2-DOF soft robotic arm. Presently we concentrated on the behavior of a single joint without the interference caused by dynamic coupling between the joints. The results of several experiments where different excitation signals were used confirmed the existence of significant hysteresis of θ - Δp relationship represented by the formation of major loop (for full-range excitation) and minor loops (for signals with higher frequencies). The formation of loops can be associated with pressure difference waveform of a given peak-to-peak value. This value can then be linked to the size of hysteresis loop in x-axis direction. If the peak-to-peak value of pressure difference waveform is held constant, the output forms a continuous minor loop. This fact can be important for applying certain hysteresis models so that unique correspondence between the pressure difference and the joint angle (or vice versa for an inverse model) is obtained. In addition to that, by using the excitation signal in the form of pulses with random duration and position in time we could observe the phenomenon of loop crossing, which attests to the non-local character of the investigated hysteresis.
In further work, we would like to concentrate on developing an inverse model of θ - Δp hysteresis using one of the available hysteresis models. In that case we would be able to uniquely identify the desired joint angle with necessary pressure difference.

ACKNOWLEDGMENTS

The research is supported by the grant of Research Grant Agency under Ministry of Education, Science, Research and Sport of the Slovak Republic and Slovak Academy of Sciences No.1/0822/16 titled "The Research of 3-DOF Intelligent Manipulator Based on Pneumatic Artificial Muscles".

REFERENCES

[Ahn 2010] Ahn, H. P. H. and Loi, L. T. Dynamic Model Identification of PAM-based Rehabilitation Robot Using Neural MIMO NARX Model. In : Proceedings of the 3rd International Conference on the Development of Biomedical Engineering, January 11-14, 2010, Ho Chi Minh City, Vietnam, 39-43

[Aschemann 2014] Aschemann, H. And Schindele, D. Comparison of Model-based Approaches to the Compensation of Hysteresis in the Force Characteristic of Pneumatic Muscles. IEEE Transactions on Industrial Electronics, Vol. 61, No.7, 3620-3629, ISSN 0278-0046

[Bergemann 2002] Bergemann, D. et al. Actuating Means. US 6349746 B1. Alexandria, Virginia : United States Patent and Trademark Office, 2002

[Bertotti 1998] Bertotti, G. Hysteresis in Magnetism. San Diego: Academic Press, 1998. ISBN 978-0-12-093270-2

[Doumit 2009] Doumit, M. et al. Analytical Modeling and Experimental Validation of the Braided Pneumatic Muscle. IEEE Transactions on Robotics, 2009, Vol.25, No.6, 1282-1291, ISSN 1552-3098

[Hildebrandt 2005] Hildebrandt, A. et al. Cascaded Control Concept of a Robot with Two Degrees of Freedom Driven by Four Artificial Pneumatic Muscle Actuators. In: Proceedings of the 2005 American Control Conference, June 8-10, 2005, Portland, Oregon, IEEE, 680-685

[Jazar 2010] Jazar, R. N. Theory of Applied Robotics. New York : Springer, 2010. ISBN 978-1-4419-1749-2

[Kecskemethy 2008] Kecskemethy, A. et al. A Fluidic-muscle Driven Force-controlled Parallel Platform for Physical Simulation of Virtual Spatial Force-displacement Laws. In: Proceedings of the Second International Workshop on Fundamental Issues and Future Research Direction for Parallel Mechanisms and Manipulators, September 21-22, 2008, Montpellier, France, IEEE, 1-8

[Kelasidi 2012] Kelasidi, E. et al. A Survey on Pneumatic Muscle Actuators Modeling. Journal of Energy and Power Engineering, 2012, Vol.6, No.9, 1442-1452, ISSN 1934-8975

[Lin 2015] Lin, Ch. J. et al. Hysteresis Modeling and Tracking Control for a Dual Pneumatic Artificial Muscle System Using Prandtl-Ishlinskii Model. Mechatronics, Vol.28, 35-45, ISSN 0957-4158

[Mayergoyz 2003] Mayergoyz, I. D. Mathematical Models of Hysteresis. New York: Elsevier Science Inc., 2003. ISBN 0-12-480873-5

[Pujana-Arrese 2010] Pujana-Arrese, A. et al. Modelling in Modelica and Position Control of a 1-DoF Set-up Powered by Pneumatic Muscles. Mechatronics, 2010, Vol.20, No.5, 535-552, ISSN 0957-4158

[Riccardi 2012] Riccardi, L. Position Control with Magnetic Shape Memory Actuators. Raleigh: Lulu Press Inc., 2012. ISBN 978-1-291-07319-5

[Schindele 2012] Schindele, D. and Aschemann, H. Model-based compensation of hysteresis in the force characteristic of pneumatic muscles. Proceedings of the 12th IEEE International Workshop on Advanced Motion Control, March 25-27, 2012, Sarajevo, Bosnia and Herzegovina, 1-6, ISBN 978-1-4577-1072-8

[Schindele 2013] Schindele, D. and Aschemann, H. Comparison of Cascaded Backstepping Control Approaches with Hysteresis Compensation for a Linear Axis with Pneumatic Muscles. In: Proceedings of the 9th IFAC Symposium on Nonlinear Control Systems, September 4-6, 2013, Toulouse, France, 773-778

[Schreiber 2012] Schreiber, F. et al. Model-based Controller Design for Antagonistic Pairs of Fluidic Muscles in Manipulator Motion Control. In: Proceedings of the International Conference on Methods and Models in Automation and Robotics, August 27-30, 2012, Miedzyzdroje, Poland, IEEE, 499-504

[Tondu 2012] Tondu, B. Modelling of the McKibben Artificial Muscle: A review. Journal of Intelligent Material Systems and Structures, Vol.23, No.3, 2012, 225-253, ISSN 1045389X

[Van Damme 2008] Van Damme, M. et al. Modeling Hysteresis in Pleated Pneumatic Artificial Muscles. In : Proceedings of the 2008 IEEE Conference on Robotics, Automation and Mechatronics, September 21-24, 2008, Chengdu, China, 471-476, ISBN 978-1-4244-1675-2

[Vo-Minh 2009] Vo-Minh, T. et al. Non-local Memory Hysteresis in a Pneumatic Artificial Muscle (PAM). In : Proceedings of the International Conference on Control and Automation, December 9-11, 2009, Christchurch, New Zealand, 640-645

[Vo-Minh 2011] Vo-Minh, T. et al. A New Approach to Modeling Hysteresis in a Pneumatic Artificial Muscle Using the Maxwell-slip Model. IEEE/ASME Transactions on Mechatronics, Vol.16, No.1, 2011, 177-186, ISSN 1083-4435

[Wickramatunge 2009] Wickramatunge, K. C. and Leephakpreeda, T. Empirical Modeling of Pneumatic Artificial Muscle. In: Proceedings of the International MultiConference of Engineers and Computer Scientists IMECS 2009, March 18-20, 2009, Hong-Kong, IEEE, 1726-1730, ISBN 978-988-17012-7-5

[Zhang 2008] Zhang, J.-F. et al. Modeling and Control of a Curved Pneumatic Muscle Actuator for Wearable Elbow Exoskeleton. Mechatronics, 2008, Vol.18, No.8, 448-457, ISSN 0957-4158

[Zhong 2014] Zhong, J. et al. One Nonlinear PID Control to Improve the Control Performance of a Manipulator Actuated By a Pneumatic Muscle Actuator. Advances in Mechanical Engineering, Vol. 2014, 2014, 1-19, ISSN 16878140

[Zhu 2008] Zhu, X. C. et al. Adaptive Robust Posture Control of Parallel Manipulator Driven By Pneumatic Muscles with Redundancy. IEEE/ASME Transactions on Mechatronics, Vol.13, No.4, 2008, 441-450, ISSN 1083-4435

CONTACTS:

Doc. ing. Alexander Hosovsky, PhD.
Technical Univesrity of Košice
Faculty of Manucaturing Technologies with Seat in Presov
Bayerova 1
08001 Presov, Slovak Republic
e-mail: alexander.hosovsky@tuke.sk
www.tuke.sk